Deletion of 5-Lipoxygenase in the Tumor Microenvironment Promotes Lung Cancer Progression and Metastasis through Regulating T Cell Recruitment

Joanna M. Poczobutt,* Teresa T. Nguyen,* Dwight Hanson,* Howard Li,*,† Trisha R. Sippel,* Mary C. M. Weiser-Evans,*,‡ Miguel Gijon,‡ Robert C. Murphy,‡ and Raphael A. Nemenoff*,‡

Eicosanoids, including PGs, produced by cyclooxygenases (COX), and leukotrienes, produced by 5-lipoxygenase (5-LO) have been implicated in cancer progression. These molecules are produced by both cancer cells and the tumor microenvironment (TME). We previously reported that both COX and 5-LO metabolites increase during progression in an orthotopic immunocompetent model of lung cancer. Although PGs in the TME have been well studied, less is known regarding 5-LO products produced by the TME. We examined the role of 5-LO in the TME using a model in which Lewis lung carcinoma cells are directly implanted into the lungs of syngeneic WT mice or mice globally deficient in 5-LO (5-LO-KO). Unexpectedly, primary tumor volume and liver metastases were increased in 5-LO-KO mice. This was associated with an ablation of leukotriene (LT) production, consistent with production mainly mediated by the microenvironment. Increased tumor progression was partially reproduced in global LTC_4 synthase KO or mice transplanted with LTA_4 hydrolase-deficient bone marrow. Tumor-bearing lungs of 5-LO-KO had decreased numbers of CD4 and CD8 T cells compared with WT controls, as well as fewer dendritic cells. This was associated with lower levels of CCL20 and CXL9, which have been implicated in dendritic and T cell recruitment. Depletion of CD8 cells increased tumor growth and eliminated the differences between WT and 5-LO mice. These data reveal an antitumorigenic role for 5-LO products in the microenvironment during lung cancer progression through regulation of T cells and suggest that caution should be used in targeting this pathway in lung cancer. ***The Journal of Immunology*****, 2016, 196: 891–901.**

Lung cancer remains the leading cause of cancer-related deaths worldwide. The main reason for the high mortality rate is that the majority of the patients present with advanced disease and metastasis at diagnosis. Although therapies targeted toward specific driver mutations in cancer cells initially achieve high response rates in select groups of patients, resistance to these agents eventually develops, and the overall 5-year survival for patients with lung cancer remains at ~15% (1). This indicates that additional strategies are needed to provide long-lasting survival benefit. Although extensive research has focused on genetic mutations in neoplastic epithelial cells, it has now become apparent that cancer progression and metastasis involve complex interactions between cancer cells and the cells of the tumor microenvironment (TME) (2, 3). In particular, the inflammatory milieu of the TME has become an important new focus of lung cancer research (4).

Bioactive lipids derived from polyunsaturated fatty acids, such as arachidonic acid, play an essential role in regulation of inflammation. Arachidonic acid is released from cellular membranes predominantly by cytosolic phospholipase A2α ($cPLA_2$) and is processed by a variety of downstream enzymes to form a family of eicosanoids. Cyclooxygenases (COX) produce PGs, including PGE_2, prostacyclin, as well as thromboxane A2. The 5-lipoxygenase (5-LO) enzyme controls another key pathway in arachidonic acid metabolism, and its major products include leukotriene B4 (LTB_4) and the cysteinyl leukotrienes: leukotriene C4 (LTC_4), leukotriene D4 (LTD_4), and leukotriene E4 (LTE_4). Other products of the 5-LO pathway include 5-hydroxyeicosatetraenoic acid, 5-oxo-eicosatetraenoic acid, lipoxins A_4 and B_4, as well as resolvins and protectins, which are derived from eicosapentaenoic or docosahexaenoic acids (5–8). Leukotrienes are potent inflammatory mediators implicated in diseases including asthma and atherosclerosis, and inhibitors of 5-lipoxygenase signaling are in clinical use as antiasthmatic agents (5). There has also been significant interest in exploring the role of the 5-LO pathway in

*Department of Medicine, University of Colorado Denver, Aurora, CO 80045; †Veterans Affairs Medical Center, Denver, CO 80220; and ‡Department of Pharmacology, University of Colorado Denver, Aurora, CO 80045

ORCIDs: 0000-0002-7211-4176 (T.T.N.); 0000-0002-1230-2941 (H.L.); 0000-0002-9430-6515 (R.C.M.).

Received for publication July 23, 2015. Accepted for publication November 9, 2015.

This study was supported by the National Institutes of Health/National Cancer Institute (Grants R01 CA162226, R01 CA164780, and R01 CA108610 to R.A.N.), Colorado Lung Cancer Specialized Programs of Research Excellence (Grant P50 CA058187), a Ruth L. Kirschstein National Research Service Award (Grant T32CA17468 to T.R.S.), and the U.S. Department of Veterans Affairs (Career Development Award 1IK2BX001282-01A1 to H.L.). The Flow Cytometry Shared Resource receives support from the National Institutes of Health/National Cancer Institute (University of Colorado Cancer Center Support Grant P30 CA046934).

Address correspondence and reprint requests to Prof. Raphael A. Nemenoff, Department of Medicine, Division of Renal Diseases and Hypertension, University of Colorado Denver, C-281, 12700 East 19th Avenue, Aurora, CO 80045. E-mail address: raphael.nemenoff@ucdenver.edu

The online version of this article contains supplemental material.

Abbreviations used in this article: COX, cyclooxygenase; $cPLA_2$, cytosolic phospholipase A2α; LC/MS/MS, liquid chromatography–tandem mass spectrometry; LLC, Lewis lung carcinoma; LLC-Luc, luciferase-expressing Lewis lung carcinoma cell; 5-LO, 5-lipoxygenase; 5-LO-KO, globally deficient in 5-LO; LTA4H-KO, leukotriene A4 hydrolase knockout; LTB_4, leukotriene B4; LTC_4, leukotriene C4; LTC4S-KO, leukotriene C4 synthase knockout; LTD_4, leukotriene D4; LTE4, leukotriene E_4; SDF-1α, stromal cell–derived factor-1α; TME, tumor microenvironment; Treg, regulatory T cell; WT, wild-type.

cancer; however, the results have been conflicting. Although pharmacological inhibitors have shown antiproliferative and proapoptotic effects in studies on cancer cells, clinical trials using these agents have not shown efficacy (9–11). In addition, these agents appear to have significant off-target effects (7). A number of studies have used a genetic approach to assess the 5-LO pathway in murine models of cancer (12–14). However, most of these studies have focused on tumor initiation rather than progression and have not distinguished between the role of 5-LO in cancer cells versus the tumor microenvironment.

We recently developed an immunocompetent orthotopic model in which murine lung cancer cells are directly implanted into the left lung lobe of syngeneic mice (15–17). These cells form a primary tumor that metastasizes to other lobes of the lung, lymph nodes, as well as liver and brain. This model presents a unique opportunity to assess the role of specific pathways selectively in the TME, by injecting wild-type (WT) mouse cancer cells into mouse hosts that carry a specific deletion of the gene of interest. To study the influence of 5-LO metabolites produced by the TME on tumor progression and metastasis, we examined lung cancer growth and progression in mice deficient in enzymes in the leukotriene pathway. Unexpectedly, these data indicate loss of 5-LO in the TME results in increased primary tumor growth and metastasis. Our data indicate that 5-LO products regulate the recruitment of cytotoxic T cells to the primary tumor, and loss of this pathway increases tumor progression.

Materials and Methods

Cells

Luciferase-expressing Lewis lung carcinoma cells (LLC-Luc) were obtained from Caliper and maintained in DMEM (#19-017-CV; Corning CellGro) containing 10% FBS, penicillin/streptomycin, and G418 (500 ng/ml).

Mice

Mice globally deficient in 5-LO (5-LO-KO) on a C57BL/6 background (strain B6.129S2-Alox5 < tm1Fun > /J) as well as WT C57BL/6 mice were obtained from The Jackson Laboratory. Mice lacking the ability to produce cysteinyl leukotrienes (LTC_4 synthase KO [LTC4S-KO]) on a C57BL/6 background and mice lacking the ability to produce LTB_4 (leukotriene A4 hydrolase KO [LTA4H-KO]) on a 129 background were a generous gift of Dr. Robert Murphy (University of Colorado). LTA4H-KO mice were backcrossed for eight generations with WT C57BL/6 mice. All mice were bred and maintained in the Center for Comparative Medicine at the University of Colorado Denver. Experiments were done in 10–16-wk-old mice, both males and females, with mice of different age and gender equally represented in all experimental groups. All procedures were performed under protocols approved by the Institutional Animal Care and Use Committee at the University of Colorado Denver.

Orthotopic mouse model

LLC-Luc cells (1×10^5 in 25 μl/injection) were suspended in PBS containing 15% Growth Factor Reduced Matrigel (#354230; BD Biosciences) and injected into the parenchyma of the left lung lobe through the rib cage using a 30-gauge needle, as previously described (16). To directly visualize the lung during injection, a 4- to 5-mm incision was made in the skin under the left shoulder, and s.c. fat was removed. After the procedure, the incision was closed using veterinary adhesive. Mice were sacrificed 2.5–4 wk after injection. At the time of sacrifice, mice were injected i.p. with 300 mg/kg body weight luciferin (Caliper) 10 min before euthanasia. Lungs and liver were harvested and immediately imaged for bioluminescence using the IVIS Imaging System 50 Series (Caliper Life Sciences/Xenogen). Two images were taken per liver (front and back), and the number of metastatic foci was added. Primary tumor size was measured using digital calipers.

Flank model

LLC-Luc cells (1×10^5 in 40 μl volume/injection) were suspended in PBS containing Matrigel as above. Cells were injected into right flanks of WT or 5-LO-KO mice, and animals were sacrificed 3 wk after injection. Primary tumors were measured with a caliper, and metastatic foci in lungs and liver were assessed by bioluminescence as described above. For this experiment, 20–30-wk-old mice were used.

Eicosanoid profiling

Mice were sacrificed at 3 wk after cancer cell injection, and the whole left lung lobe containing the tumor was excised, weighed, and flash-frozen in liquid nitrogen. Tissues were further processed and analyzed by liquid chromatography–tandem mass spectrometry (LC/MS/MS) as previously described (16). Results were normalized to total protein.

Preparation of single-cell suspension and flow cytometry

Mice were sacrificed at 2.5 wk after cancer cell injection, and the circulation was perfused with PBS/heparin (20 U/ml; Sigma-Aldrich). Whole left lung lobes containing tumors were excised and weighed, and tumors were measured with an electronic caliper. Spleens were collected from the same mice and processed using the same protocol as lungs. Individual lungs were mechanically dissociated with scissors and incubated for 30 min at 37°C with 3.2 mg/ml collagenase type 2 (43C14117B; Worthington), 0.75 mg/ml Elastase (33S14652; Worthington), 0.2 mg/ml Soybean Trypsin Inhibitor (S9B11099N; Worthington), and DNAse I 40 μg/ml (Sigma-Aldrich). During incubation, samples were placed in a shaking water bath and dispersed by pipetting every 10 min. Resulting single-cell suspensions were filtered through 70-μm cell strainers (BD Biosciences) and washed with staining buffer (PBS containing 1% FBS, 2 mmol EDTA, and 10 mmol HEPES). Samples were subject to RBC lysis, washed with staining buffer, and filtered through 40-μm cell strainers (BD Biosciences). Prior to staining, FcγR was blocked with anti-CD16/CD32 Ab (BD Biosciences) for 10 min. Cells were stained for 30–45 min at 4°C with the following Abs: CD11b-FITC (clone M1/70; BD Biosciences), Siglec F–PE or Alexa Fluor 647 (clone E50-2440; BD Biosciences), Ly6G-PE–Cy7 (clone 1A8; BD Biosciences), CD64-PE or Alexa Fluor 647 (clone X54-5/7.1; BD Biosciences), CD11c-allophycocyanin–Cy7 (clone HL3; BD Biosciences), CD11c-PerCP–Cy5.5 (clone N418, BioLegend), CD3-PE–Cy7 (clone 145-2C11; BD Biosciences), CD4-APC–Cy7 (clone GK1.5; BioLegend), CD8-APC (clone 53-6.7; BioLegend), and NK1.1-PE (clone PK136; BioLegend).

For the evaluation of Th1/Th2 cells, tumor-bearing lungs from WT and 5-LO-KO mice 3 wk after LLC cell injection were harvested and processed into single-cell suspension as described above. Spleens were harvested from the same mice and mechanically dissociated. Cells were incubated (1 h, 4°C) with the following Abs: CD4 (clone GK1.5; eBioscience), CXCR3 (CXCR3-173; eBioscience), CD3 (145-2C11; eBioscience), and CD45 (30-F11; eBioscience). LIVE/DEAD Fixable Aqua Dead Cell Stain Kit (#L34965; Molecular Probes) was used to stain dead cells. Following a wash, the cells were fixed and permeabilized (4°C, overnight) using the Foxp3 Staining Buffer Set (#00-5523-00; eBioscience) and incubated (2 h, 4°C) with the following intracellular stain Abs: Gata-3 (TWAJ; eBioscience) and T-bet (O4-46; BD Biosciences).

For regulatory T cell (Treg) evaluation, lungs from a separate group of tumor-bearing WT and 5-LO-KO mice was harvested, and tissues were processed as described above. Cells were stained (1 h, 4°C) with the following Abs: CD45 (clone F30-11; BioLegend), CD3 (145-2C11; BD Biosciences), CD4 (clone GK1.5; BioLegend). Following a wash, cells were fixed and permeabilized using Mouse Foxp3 Buffer Set (#560409; BD Pharmingen) per the manufacturer's instructions. Intracellular staining (0.5 h, 4°C) was performed with Foxp3 (clone FJK-16s; eBioscience).

Cells were analyzed at the University of Colorado Cancer Center Flow Cytometry Core Facility using a Gallios Flow Cytometer (Beckman Coulter). The analysis strategy involved excluding debris and cell doublets by light scatter and dead cells by DAPI (1 μg/ml). Data were analyzed using Kaluza Software (Beckman Coulter).

Quantitative real-time-PCR

Tumor-bearing left lung lobes were frozen in liquid nitrogen immediately after harvest and then homogenized in RLT Plus buffer (Qiagen) using a motor-driven homogenizer. Total RNA was isolated using an RNeasy Plus Mini Kit (Qiagen). Reverse transcription was performed using an iScript cDNA Synthesis Kit (Bio-Rad). Real-time PCR was conducted on MyIQ Real Time PCR Detection System (Bio-Rad) using Power SYBR Green PCR Master Mix (Applied Biosystems). The relative message levels of each gene were normalized to 18S. The following primers were used: CCL20: forward 5′-GCCTCTCGTACATACAGACGC-3′ and reverse 5′-CCAGTTCTGCTTTGGATCAGC-3′; CXCL9 forward 5′-TCAACAAAAGAGCTGCCAAA -3′ and reverse 5′-GCAGAGGCCAGAAGAGAGAA-3′;

CXCL10: forward 5′-CCAAGTGCTGCCGTCATTTTC-3′ and reverse 5′-GGCTCGCAGGGATGATTTCAA-3′; granzyme B: forward 5′-CATGCTGCTAAAGCTGAAGAGT-3′ and reverse 5′-TTCCCCAACCAGCCACATAG-3′; IFN-γ: forward 5′-GGAACTGGCAAAAGGATGGTG-3′ and reverse 5′-ATGTTGTTGCTGATGGCCTG-3′; MCP-1: forward 5′-CACTCACCTGCTGCTACTCA-3′ and reverse 5′-GCTTGGTGACAAAAACTACAG-3′; stromal cell–derived factor-1α (SDF-1α): forward 5′-CCTTCAGATTGTACGGC-3′ and reverse 5′-CTTGCATCTCCCACGGATGT-3′; and 18s: forward 5′-CGCCGCTAGAGGTGAAATTC-3′ and reverse 5′-TTGGCAAATGCTTTCGCTC-3′.

Immunohistochemical staining

After sacrifice, the mouse circulation was perfused with heparinized PBS (20 U/ml), and the lungs were inflated with PBS containing 4% paraformaldehyde. The heart and lung blocks were removed and fixed in 4% paraformaldehyde (20 h). Cryopreservation was carried out in 15% sucrose (24 h), followed by 30% sucrose (48 h), and a 1:1 mixture of OCT and 30% sucrose (24 h). Tissues were embedded in OCT (Sakura), frozen, and cut into 6-μm sections.

For immunostaining, sections were thawed and washed in deionized water. Ag retrieval was carried out in a Decloaking Chamber (Biocare Medical) for 20 min at 100°C using Borg Decloaker RTU solution (Biocare Medical). After cooling, sections were washed in deionized water and transferred to TBST (0.05 mol Tris, 0.15 mol NaCl, and 0.1% v/v Triton X-100 [pH 7.6]). Sections were sequentially incubated with 3% hydrogen peroxide (10 min), avidin, and biotin blocking solutions (Vector Laboratories), 15 min each, blocking solution (1:1 solution of 3% normal goat serum; Vector Laboratories), and Super Block (SkyTek Laboratories) for 1 h at room temperature. Slides were incubated with rabbit anti-CD31 polyclonal Ab (#ab28364, 1:50; Abcam) or rat anti-F4/80 mAb (MF48000; 1:100; Life Technologies) or rabbit anti-mouse CD3 polyclonal Ab (ab49942, 1:100; Abcam) at 4°C overnight, followed by washes in TBST, biotinylated anti-rabbit or anti-rat secondary Ab (Vector Laboratories) for 30 min at room temperature, and Vectastain ABC reagent (Vector Laboratories) for 30 min. Ag was visualized using diaminobenzidine substrate, and nuclei were counterstained with Harris hematoxylin.

Immunohistochemistry quantitation

To assess microvessel density, three sections from each animal were stained for CD31, and the three most vascularized areas (hot spots) within each tumor section were chosen at low magnification. In each of these three areas, vessels were counted in a representative high-magnification field (×40), with single CD31-positive endothelial cells or endothelial cell clusters counted as individual microvessels (18). Counts were performed independently by two blinded observers, and mean microvessel density was calculated as the average count per high-power field. In a similar way, CD3 was quantified in the "hot spots" in the sections. To assess the macrophage population in mouse lung tumors, one section per animal for four mice per WT or 5-LO KO group were stained for F4/80. Three areas of the lung tumor section were examined: the uninvolved lung, the tumor edge, and inside the tumor. Ten ×40 magnification fields were randomly chosen for each area, and the F4/80-positive cells were counted.

CD8 depletion

Mice were injected i.p. with 200 μg anti-CD8a Ab (clone 53-6.27, #BE004-1; BioXCell) or isotype control (clone 2A3, #BE0089; BioXCell) every 5 d, starting 1 d prior to cancer cell injection. Cancer cells (LLC-Luc) were injected as described above, and tumors were harvested 18 d postinjection.

Bone marrow transplant

For bone marrow transplants, LTA4H-KO and WT donor mice on a C57BL/6 background were sacrificed, femurs and tibias were aseptically removed, and bone marrow obtained by aspiration. Cells were suspended in sterile HBSS. Recipients, 9-wk-old WT C57BL/6 mice were irradiated (850 rad; split dose) by RS200 x-ray source. One hour following the second dose, isoflurane-anesthetized recipients were injected with donor marrow via retro-orbital injection (2×10^6 bone marrow cells/mouse). After transplantation, mice were maintained on antibiotic chow for 1 wk and allowed to engraft donor bone marrow for 8 wk prior to experimentation.

Statistics

Statistical analyses were conducted using GraphPad Prism software (GraphPad). Differences were identified using Student two-tailed *t* test, and $p < 0.05$ was considered significant.

Results

5-LO deficiency in the tumor microenvironment increases primary tumor growth and liver metastasis

We have developed an immunocompetent orthotopic model in which murine lung cancer cells are directly implanted into the left lung lobe of syngeneic mice (15–17). These cells form a primary tumor that, over a period of 3–5 wk, metastasizes to distant organs including the liver and brain. To elucidate the role of 5-LO expressed in the microenvironment in lung cancer progression and metastasis, we injected LLC-Luc cells into syngeneic C57BL/6 mice globally deficient in 5-LO (5-LO-KO), in parallel with WT C57BL/6 mice. With this strategy, 5-LO was selectively deleted in the TME (host cells). The WT 5-LO gene was maintained in the injected LLC-Luc cancer cells; however, we showed that these cells do not produce any leukotrienes in vitro (16). Mice were sacrificed 3 wk after cancer cell injection, and left lung lobes with tumors were harvested. To assess liver metastases, we took advantage of luciferase expression in LLC-Luc cells, which allows for detection of cancer cells in distant organs by ex vivo bioluminescence imaging.

As shown in Fig. 1A, the median primary tumor volume in 5-LO-KO mice was >2-fold larger than in WT mice. Liver metastases were detected in all of the mice; however, in the 5-LO-KO mice, the median number of metastatic foci per liver was 2-fold higher than in WT mice (Fig. 1B, 1C). Additionally, we tested tumor growth and metastasis in flank injection model. In agreement with the orthotopic model, in this experiment, we detected increased primary tumor growth and a trend toward increased metastasis to the liver and the lung in 5-LO-KO mice, compared with WT mice (Fig. 1D).

Eicosanoid profiles in tumor-bearing lungs of 5-LO-KO mice

We have previously shown that during lung cancer progression, eicosanoid production in tumor-bearing lungs is significantly increased. Furthermore, using $cPLA_2$-KO mice in our orthotopic model, we showed that a large contribution to this increased eicosanoid production is derived from the TME, particularly in the case of leukotrienes (16). To define eicosanoid profiles in the setting of selective 5-LO deficiency in the TME, we harvested tumor-bearing lungs from 5-LO-KO and WT mice 3 wk after the injection of LLC-Luc cells and measured eicosanoid levels by LC/MS/MS. The analysis of eicosanoid profiles shows high levels of all four leukotrienes (LTB_4, LTC_4, LTD_4, and LTE_4) in tumor-bearing WT mice, whereas in 5-LO-KO hosts leukotriene production was completely abrogated (Fig. 2A). 5-Hydroxyeicosatetraenoic acid, which is also a product of 5-LO, was reduced by 50% in 5-LO-KO mice (Fig. 2A). Interestingly, deletion of 5-LO in the TME resulted not only in reduction of 5-LO pathway products, but we also found a trend toward increased PG production. That is, PGE_2 was increased by 1.5-fold, and PGD_2 by 2-fold. Although these changes did not achieve statistical significance, there was a consistent trend toward increased production of COX-derived metabolites in 5-LO-KO mice (Fig. 2B).

Analysis of myeloid cells and T cells in tumors

The TME is composed of multiple cell types, including vascular cells, fibroblasts, and cells of the immune system. Leukotrienes have been shown to play a significant role in recruitment and activation of inflammatory cells and T lymphocytes in various disease settings (19). To examine if the deficiency of 5-LO in the tumor microenvironment leads to changes in lymphocytes or inflammatory cells during tumor progression, we harvested tumor-bearing lungs from 5-LO-KO and WT mice 2.5 wk after the injection of LLC-Luc cells and analyzed cell numbers by flow cytometry.

To analyze myeloid cells in tumor bearing-lungs, we used a modification of our previously published gating strategy, which was

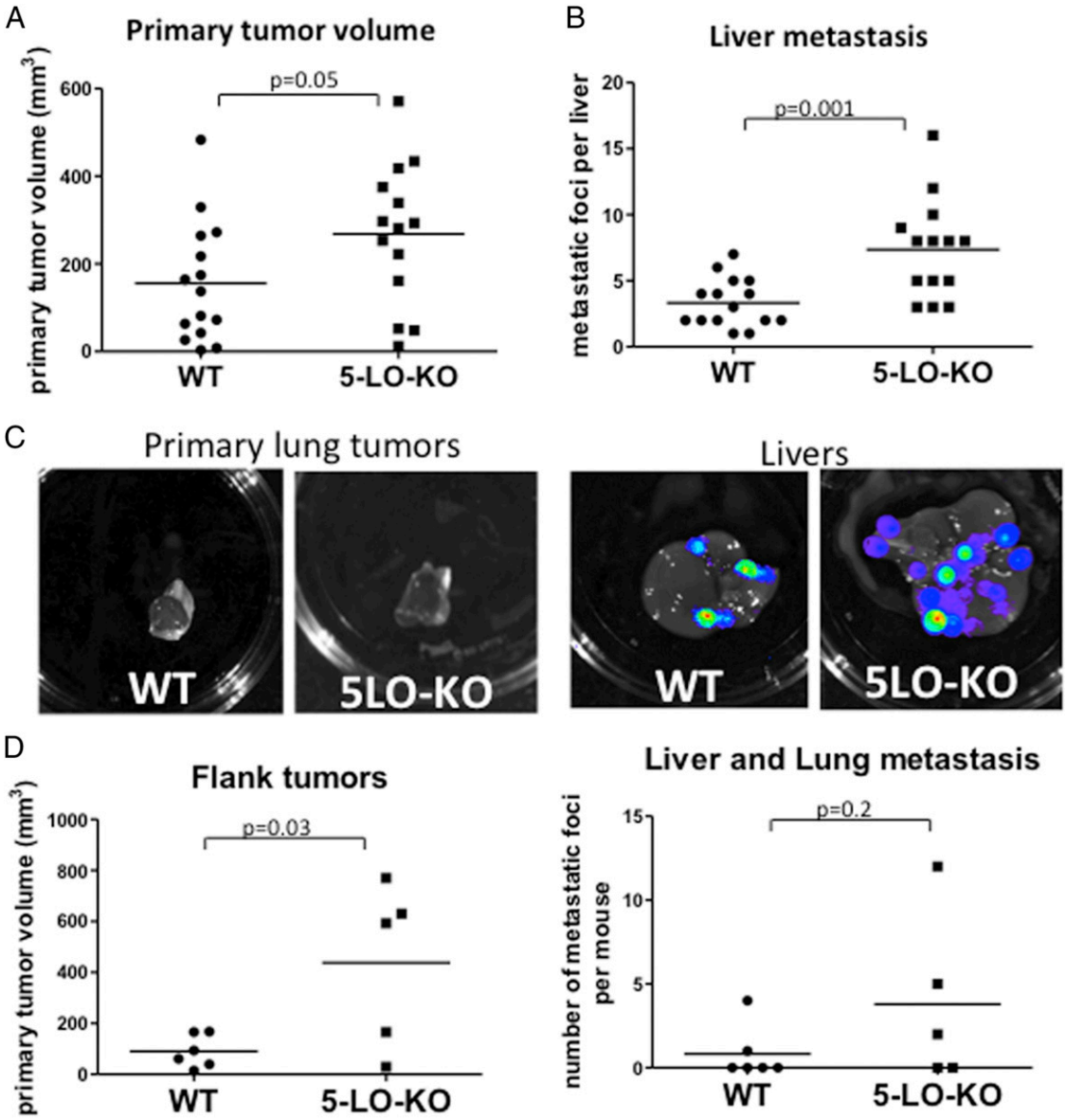

FIGURE 1. 5-LO deficiency in the tumor microenvironment increases primary tumor growth and liver metastasis burden. Murine lung adenocarcinoma cells, LLC-Luc, which possess the WT 5-LO gene and were engineered to express luciferase, were injected directly into the left lung lobe of syngeneic WT or 5-LO-KO mice. Animals were sacrificed 3 wk after injection. Prior to euthanasia, mice were injected with luciferin, and metastases were visualized by bioluminescence in excised organs. Primary tumor was measured using digital caliper. Data represent two separate experiments. Each dot represents a single mouse. Bars indicate mean levels. (**A**) Primary tumor volumes. (**B**) Number of metastatic foci per liver. (**C**) Bioluminescent images of livers with high metastatic burden in WT or 5-LO-KO mice. (**D**) Flank injection model. LLC-Luc cells were injected in flanks of WT and 5-LO-KO mice and sacrificed 3 wk after injection. *Left panel*, Primary (flank) tumor volumes measured by caliper. *Right panel*, Combined number of lung and liver metastatic foci per mouse, measured by bioluminescence after organ harvest.

based on markers commonly used to characterize inflammatory cells in the lung (16, 20–22). As shown in Fig. 3A, we identified neutrophils ($CD11b^+/Ly6G^+$), and two populations of macrophages, designated as MacA ($SigF^+/CD11c^+/CD64^+$) and MacB ($SigF^-/Ly6G^-/CD11b^+/CD64^+$). According to previous studies, MacA represent resident alveolar macrophages, whereas MacB comprise a heterogeneous population of interstitial and infiltrating macrophage/monocyte cells (21, 22). Our previously published work demonstrated that both neutrophils and MacB cells were increased in the setting of tumor in WT mice as compared with naive mice, whereas we detected no change in the number of MacA cells (16). Examination of tumors implanted in 5-LO-KO mice revealed no significant changes in the numbers of these populations in the whole tumor-bearing left lung compared with tumors in WT mice (Fig. 3B). Using immunohistochemistry to detect F4/80-positive cells, we examined whether there were differences in the localization of macrophages in the tumors. Although there were no differences in the number of F4/80 positive cells at the tumor edge or in the uninvolved lung, we consistently detected more F4/80-positive cells in the center of tumors in 5-LO-KO mice compared with WT controls (Fig. 3C, 3D). The significance of these changes remains to be determined.

In addition to inflammatory cells, we examined changes in T cell populations. Using the gating strategy shown in Fig. 4A, we assessed NK cells ($NK1.1.^+/CD3^-$), $CD4^+$ T lymphocytes ($CD3^+/CD4^+$), and $CD8^+$ T lymphocytes ($CD3^+/CD8^+$). Compared to WT mice, we detected decreases in total CD3-positive cells in tumor bearing lungs of 5-LO-KO mice, which was reflected in

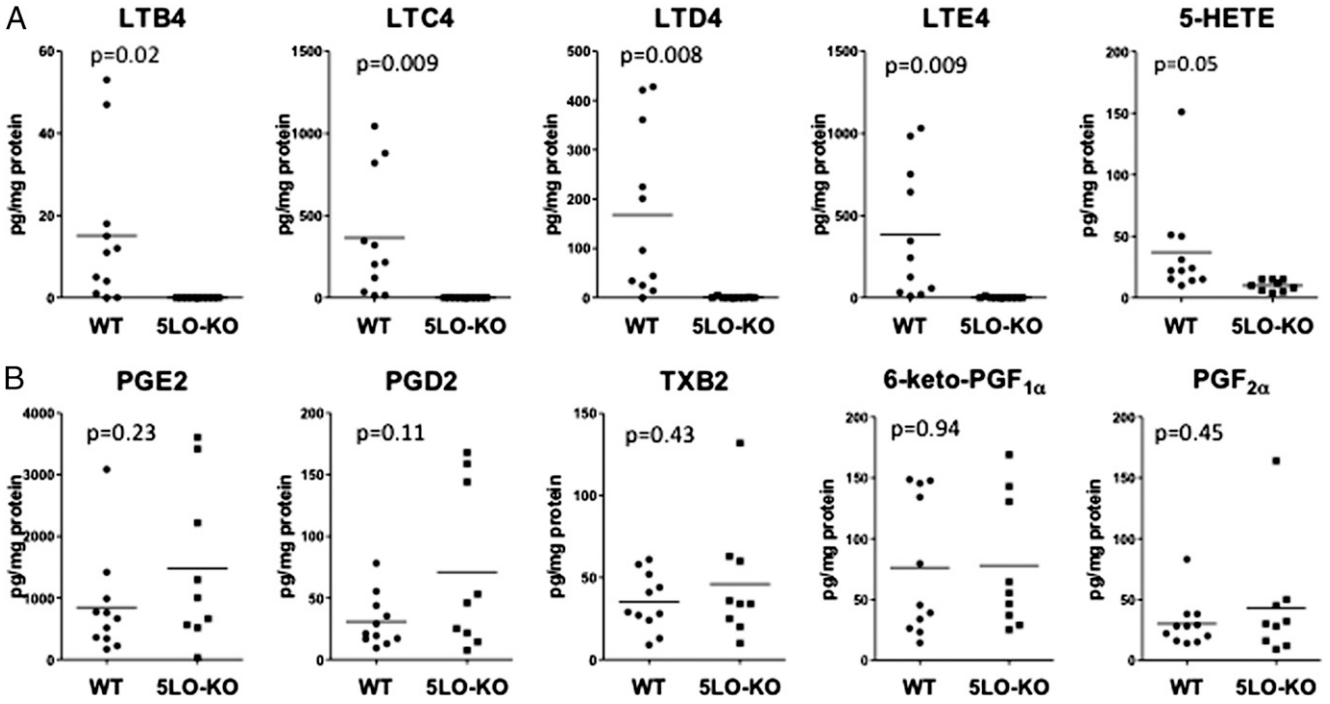

FIGURE 2. Expression of 5-LO in the microenvironment is required for the production of leukotrienes in tumor-bearing lungs. WT and 5-LO-KO mice were implanted in the left lung with LLC-Luc cells and sacrificed 3 wk after injection. Eicosanoids were extracted from tumor-bearing left lungs, quantified by LC/MS/MS, and normalized to the protein content of the sample. Bars indicate the mean level. Each dot represents a single mouse. (**A**) Products of the 5-LO pathway. (**B**) Products of the COX pathway.

decreases in both CD4 and CD8 cells (Fig. 4B). We also detected decreases in dendritic cells and NK cells (Fig. 4C). The decrease in CD3 cells was confirmed by immunohistochemistry and counting CD3-positive cells in tissue sections (Fig. 4D).

We examined the expression of a panel of cytokines/chemokines implicated in recruitment of immune and inflammatory cells in whole tumor-bearing lungs using quantitative RT-PCR. We observed marked decreases in CCL20, CXCL9, and CXCL10 expression in tumors grown in 5-LO-KO mice compared with WT controls (Fig. 5A). These molecules have been implicated in recruitment of dendritic cells and T cells, consistent with our data showing fewer of these cell populations in 5-LO tumors. We also observed decreased levels of granzyme B and IFN-γ in these tumors, consistent with decreased cytotoxic T cell function. Levels of two chemokines implicated in recruitment of myeloid cells, SDF-1α and MCP-1, were not different in WT or 5-LO-KO implanted tumors, consistent with no detectable differences in myeloid populations as measured by flow cytometry.

The increase in tumor growth rate in 5-LO-KO mice is dependent on CD8 cells

Based on these analyses, we hypothesized that the enhanced growth of tumors in 5-LO-KO mice was a result of an impaired T cell recruitment, resulting in fewer cytotoxic CD8 cells. To test this, we examined tumor progression in 5-LO-KO mice and WT controls in the setting of CD8 cell depletion. Mice implanted with cancer cells were treated every 5 d with anti-CD8 Ab or isotype control, and tumors were harvested after 2.5 wk. As shown in Fig. 5B, CD8 depletion increased primary tumor size in both WT and 5-LO-KO mice, indicating that these cells play a critical role in controlling lung cancer progression in this model. Importantly, the difference in primary tumor size between WT and 5-LO tumors was abolished in the setting of CD8 depletion, indicating that alterations in T cells underlie the increased rates of progression seen in the 5-LO-KO mice. To examine whether the deletion of 5-LO primarily affects the recruitment of T cells to tumor site or affects the overall T cell generation in these mice, we examined the numbers of these cells in the spleen. We found no significant differences in T cell populations in the spleens of WT or 5-LO-KO mice (Supplemental Fig. 1).

Although our data support a model in which the increased tumor progression in 5-LO-KO mice is due to decreased cytotoxic CD8 T cell recruitment, Tregs as well as Th2 CD4 cells have also been shown to influence tumor progression in various settings. We therefore examined Tregs as wells as Th1/Th2 markers in tumor-bearing lungs. We detected no significant differences in these populations between WT and 5-LO-KO mice (Supplemental Figs. 2, 3).

Role of cysteinyl leukotrienes and LTB_4 in cancer progression

To dissect the role of downstream products of the 5-LO pathway in cancer progression, we first assessed the role of the cysteinyl leukotrienes. We compared progression and metastasis of implanted cancer cells in LTC4S-KO mice to WT control mice. The LTC4S-KO mice will fail to produce LTC_4, LTD_4, and LTE_4, but retain 5-LO expression and can produce LTB_4 and lipoxins. Primary tumor growth showed a trend toward increase (30%) but liver metastases were not altered in LTC4S-KO mice compared with controls (Fig. 6A). To specifically examine the role of LTB4, we used LTA4H-KO mice. These mice will produce cysteinyl leukotrienes, but will not produce any LTB_4. In these studies, we determined rates of tumor progression in mice that were transplanted with LTA4H-KO bone marrow or WT bone marrow. As shown in Fig. 6B, whereas primary tumor growth was not different in LTA4H-KO compared with WT controls, there was a trend to increased liver metastasis (by 50%). These data show that LTC4S-KO or LTA4H KO in bone marrow–derived cells each partially recapitulate the effects of 5-LO-KO, with LTB_4 playing a role in the control of metastasis.

Angiogenesis

Although our data indicate that the increased lung cancer progression in 5-LO-KO mice is mediated primarily through CD8

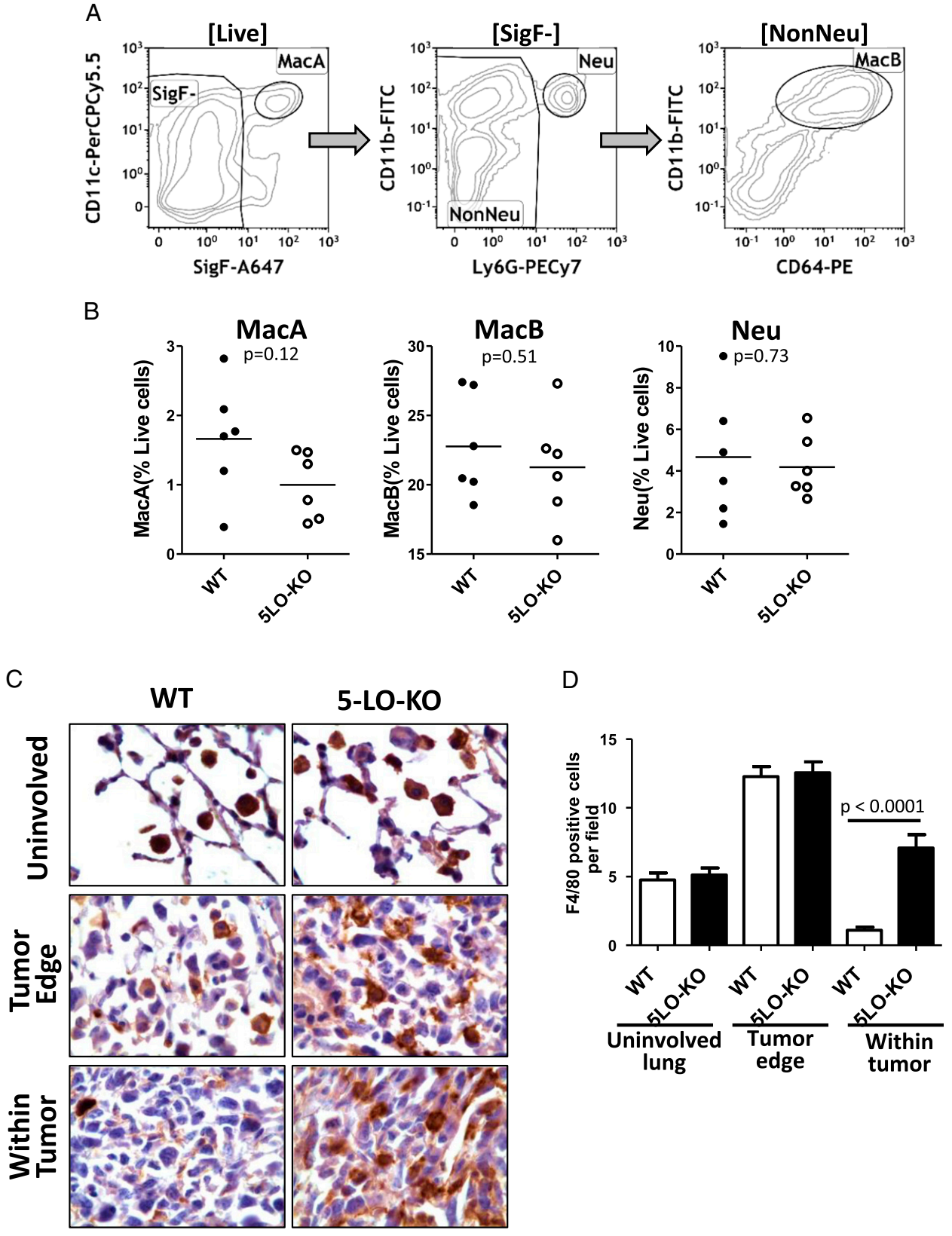

FIGURE 3. The numbers of myeloid cells in tumor-bearing lungs are not affected by 5-LO deficiency in the TME. (**A**) Sequential flow cytometry gating strategy to identify myeloid subsets in the lung: MacA macrophages ($SigF^+/CD11c^+$), neutrophils (Neu, $CD11b^+/Ly6G^+$), and MacB macrophages ($SigF^-/Ly6G^-/CD11b^+/CD64^+$). (**B**) WT and 5-LO-KO mice were implanted in the left lung with LLC-Luc cells and sacrificed after 2.5 wk. Single-cell suspensions were prepared from tumor-bearing left lobes and the numbers of macrophages (MacA and MacB) and neutrophils analyzed by flow cytometry. Each dot represents a single mouse. Data represent three independent experiments. (**C**) Macrophage localization in tumor-bearing lungs from WT and 5-LO-KO mice was analyzed by immunohistochemistry using F4/80 as a macrophage marker. Original magnification ×100. (**D**) Quantification of F4/80-positive cells in uninvolved lung, on the tumor edge, and within the tumor, expressed as the number of positive cells per ×100 field. Sections from four mice per group were counted.

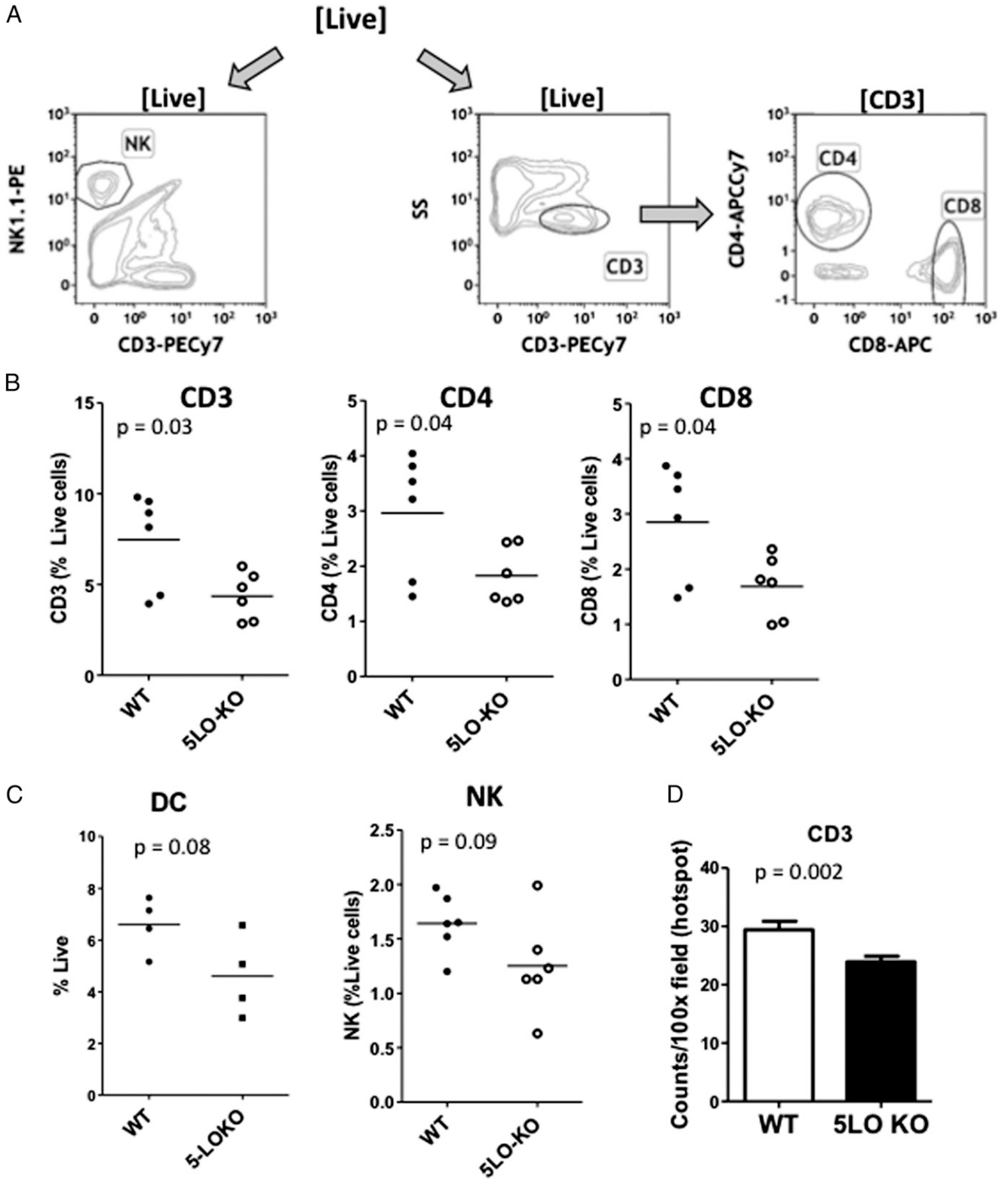

FIGURE 4. The numbers of lymphocytes in tumor-bearing lungs are decreased in the setting of 5-LO-KO in the TME. (**A**) Sequential flow cytometry gating strategy to identify lymphocytes in tumor-bearing lungs: NK cells (NK $1.1^{+}/CD3^{-}$), CD3 cells ($CD3^{+}/SSC^{Low}$), CD4 cells ($CD3^{+}/CD4^{+}$), and CD8 cells ($CD3^{+}/CD8^{+}$). (**B**) Flow cytometry–based quantitation of CD3, CD4, and CD8 cells in tumor bearing lungs from WT and 5-LO-KO mice, harvested 2.5 wk after LLC-Luc cells injection. Each dot represents a single mouse. Data represent three separate flow analyses. (**C**) Quantitation of NK cells and dendritic cells (DC). DC were identified using myeloid marker panel ($CD11c^{Hi}$/MHC class $II^{Hi}/SigF^{-}$). (**D**) Number of CD3-positive cells was assessed by immunohistochemistry. Quantification was performed in sections from six WT and four 5-LO-KO mice.

cells, we examined additional potential mechanisms. Because some 5-LO metabolites have been implicated in limiting neovascularization (23), we hypothesized that the deficiency of 5-LO would lead to increased angiogenesis in lung tumors. To examine angiogenesis, we quantified the microvessel density in histological sections of tumors harvested from WT and 5-LO-KO mice using

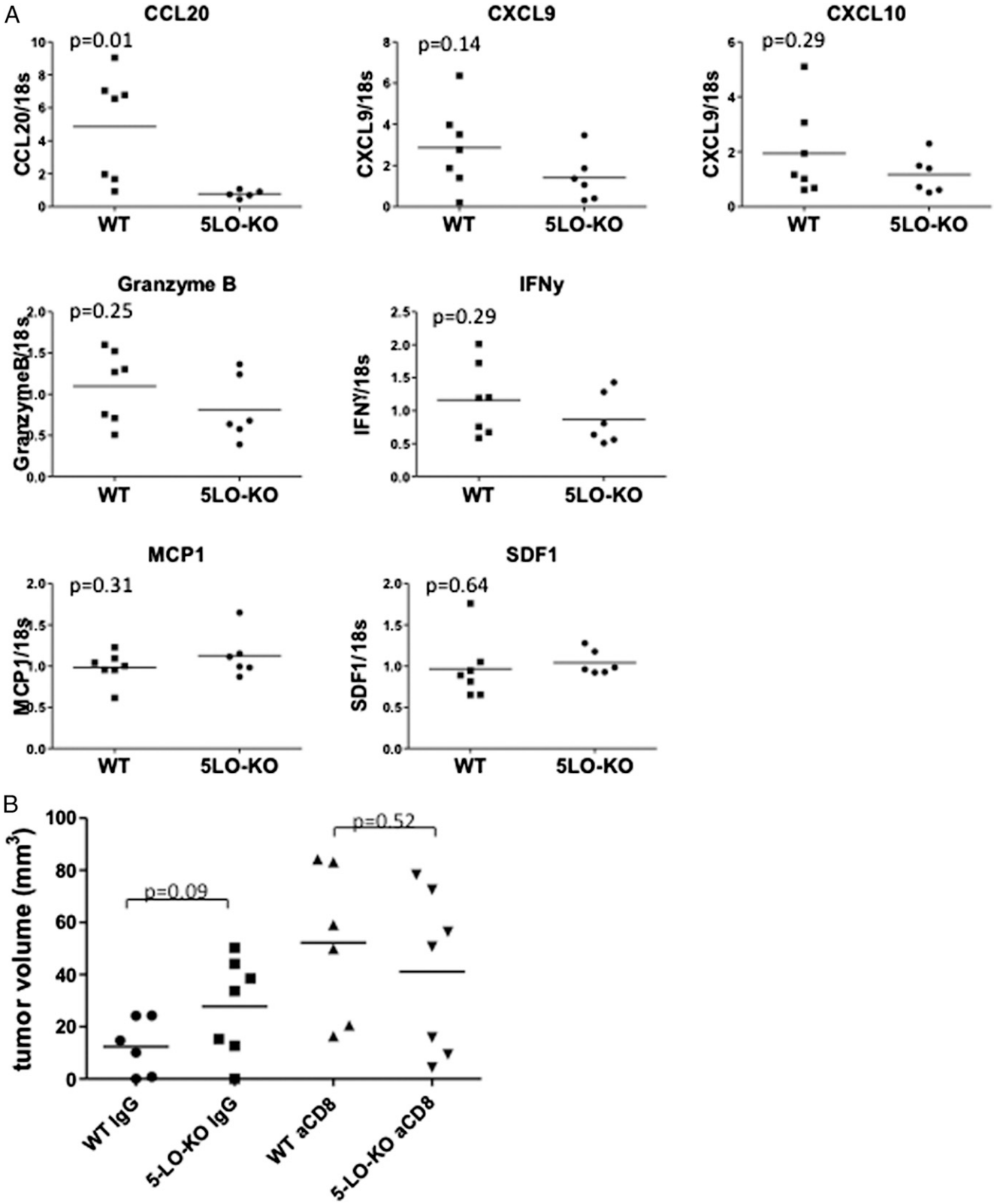

FIGURE 5. The increase in tumor growth rate in 5-LO-KO mice is dependent on CD8 cells. (**A**) Decreased expression of lymphocyte-chemoattractant chemokines in tumor-bearing lungs from 5-LO-KO mice. WT and 5-LO-KO mice were implanted in the left lung with LLC-Luc cells and sacrificed 3 wk after injection. Tumor-bearing lungs were snap-frozen and homogenized, and RNA was extracted. Expression levels of CCL20, CXCL9, CXCL10, granzyme B, IFN-γ, MCP-1, and SDF-1 were assessed by quantitative RT-PCR and normalized to 18S. (**B**) Effects of CD8 cell depletion. WT and 5-LO-KO mice were injected directly in the left lung with LLC-Luc cells and treated with anti-CD8 Ab or isotype control. Tumors were excised 2.5 wk after injection and measured with electronic calipers.

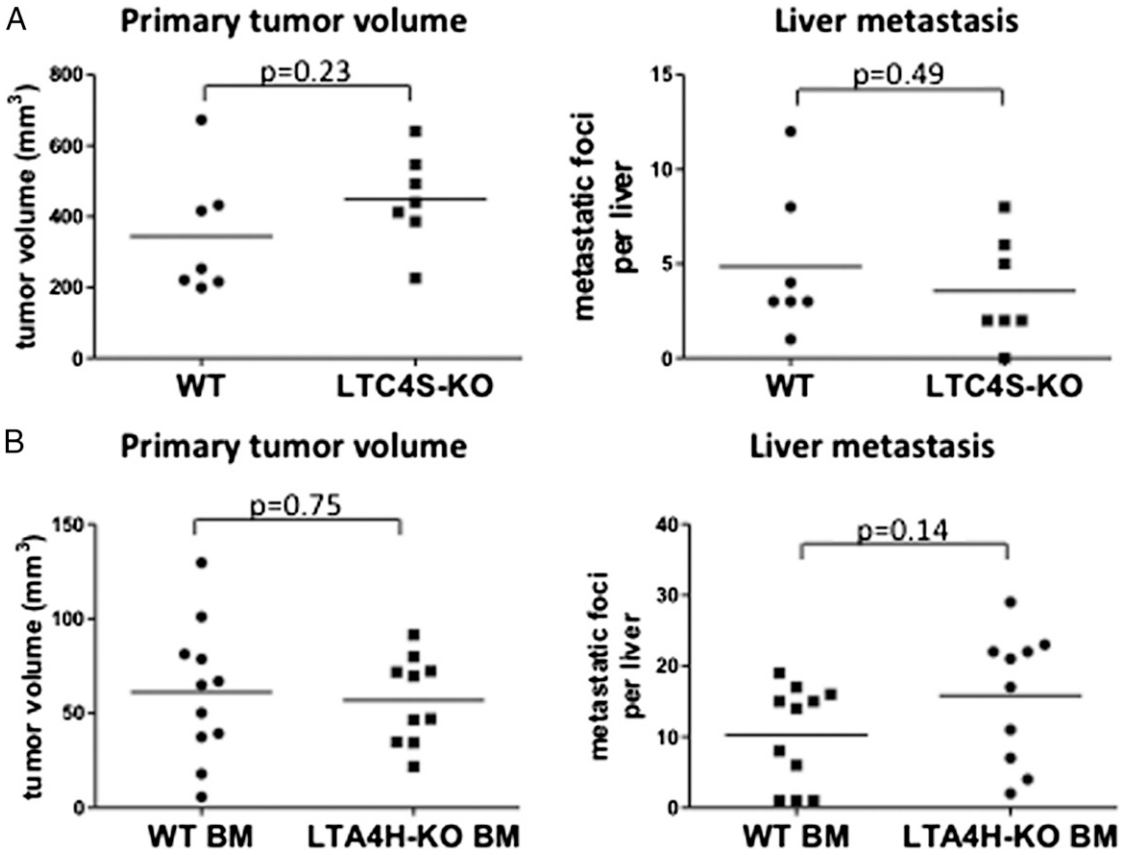

FIGURE 6. The role of cysteinyl leukotrienes and LTB_4 in cancer progression. (**A**) LLC-Luc cancer cells were injected in the left lung lobe of LTC4S-KO or WT mice. Animals were sacrificed 4 wk after injections. Tumor-bearing lungs were excised and the tumor volume was measured by a caliper. Prior to euthanasia, mice were injected with luciferin to enable visualization of metastatic foci by bioluminescence. Each dot represents a single mouse. *Left panel*, Tumor volumes; *right panel*, metastatic foci in the liver. (**B**) WT mice were irradiated and transplanted with bone marrow (BM) from LTA4H-KO or WT donors. Eight weeks after transplantation, mice were injected with LLC-Luc cancer cells. Three weeks post–cancer cell injection, animals were sacrificed for tumor growth and metastasis assessment (as above). Data represent mice from two separate injections of cancer cells. *Left panel*, Tumor volumes; *right panel*, metastatic foci in the liver.

CD31 as a marker of vascular endothelium. As shown in Fig. 7, we indeed observed a trend toward increased vessel counts in tumors growing in 5-LO-KO mice.

Discussion

Eicosanoids have been implicated as important mediators of cancer initiation, progression, and metastasis (7, 24). This family of lipid-signaling molecules contains >100 members (25) that are produced in a cell-specific and time-dependent fashion. Although extensive studies have demonstrated protumorigenic effects of COX-derived products such as PGE_2, data from our laboratory (26) and others (27) indicate that other eicosanoids inhibit cancer progression. For the 5-LO pathway, early reports pointed to its protumorigenic role, showing that pharmacological inhibition of 5-LO suppresses tumor cell growth, and addition of 5-LO products to cultured tumor cells increases proliferation and activates anti-apoptotic pathways (7, 28–31). However, these studies have been criticized for using non–physiologically relevant doses and inducing off-target effects (reviewed in Ref. 7). In contrast, clinical data so far do not support a protumorigenic role of 5-LO (9–11). In particular, a trial in advanced non–small cell lung cancer demonstrated a statistically significant decrease in the overall survival of patients treated with an LTB_4 receptor antagonist plus chemotherapy compared with patients treated with chemotherapy alone. This implies, unexpectedly, that 5-LO products were protective in this setting (11).

In the current study, mice globally deficient in 5-LO were implanted with LLC cells, which retain the 5-LO gene, but do not produce any 5-LO metabolites in vitro (16). This model allowed us to specifically examine the role of 5-LO in the TME. Our data show that the deletion of 5-LO selectively in the host increased both primary tumor size, as well as secondary metastases. Using LC/MS/MS, we detected high levels of all four leukotrienes in the WT mice with tumor, whereas in the setting of 5-LO KO in the TME, leukotriene production was completely inhibited, indicating that in this model leukotrienes are produced by the cells of the TME, rather than by the cancer cells themselves.

Our data support a model in which specific 5-LO products inhibit cancer progression and metastasis. We propose that these products do not act directly on the cancer cell but rather modify the immune response. Immune surveillance and direct cancer cell killing by cytotoxic $CD8^+$ lymphocytes in the TME is essential for generation of antitumor immunity and suppression of tumor growth. Our results show decreased numbers of dendritic cells and both CD4 and CD8 lymphocytes in the setting of 5-LO KO in the tumor microenvironment. Consistent with this, the analysis of gene expression in tumors shows lower levels of lymphocyte-chemoattractant chemokines CXCL9 and CXCL10 and lower levels of cytotoxic lymphocyte products IFN-γ and granzyme B. In contrast, the chemokines that attract myeloid cells, MCP-1 and SDF-1, were not changed in the setting of 5-LO deletion. Furthermore, treatment of tumor-injected mice with a CD8 cell–neutralizing

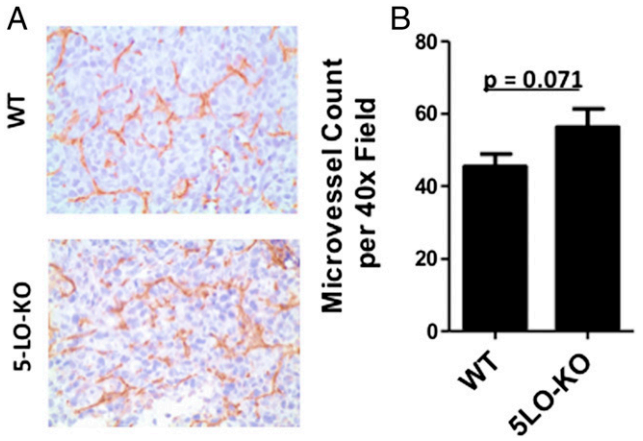

FIGURE 7. 5-LO deficiency in TME leads to increased microvessel formation. Left lung lobes were harvested from WT and 5-LO-KO mice 3 wk after injection of LLC-Luc cancer cells. Microvessel density in histological sections of tumors was assessed using CD31 as a marker of vascular endothelium and quantified as described in *Materials and Methods*. (**A**) Representative images of sections from WT and 5-LO-KO mice (original magnification ×40). Brown stain indicates CD31 Ag. (**B**) Quantification of microvessel density.

Ab led to increased primary tumor size, indicating that CD8 cells play a key role in suppressing tumor growth in our model. What is most important is that in the setting of CD8 cell neutralization, the difference in tumor growth between 5-LO-KO versus WT mice was abolished. This result demonstrates that 5-LO pathway protects against cancer progression via a mechanism that is dependent on CD8 cells. Although studies in preclinical models are not always applicable to human lung cancer, our data are consistent with the failure of inhibitors of 5-LO pathways in clinical trials (11).

To identify specific 5-LO products regulating cancer progression, we focused on cysteinyl leukotrienes and LTB_4. In mice deficient in LTC4S or in the setting of LTA4H KO in bone marrow–derived cells, we observed only partial effects on tumor progression compared with global 5-LO KO, with LTB_4 playing a role in the control of metastasis. This suggests that multiple 5-LO metabolites are important in increasing tumor progression in this model.

Our results are in concordance with previous studies examining the role LTB_4. It has been established that effector $CD8^+$ T cells highly express BLT1, the receptor for LTB_4, and can be recruited to the sites of inflammation by LTB_4 (32–34). In the setting of cancer, a study using a syngeneic s.c. cervical cancer mouse model showed accelerated tumor growth and reduced survival of $BLT1^{-/-}$ mice compared with WT mice. This study determined that the expression of BLT1 on cytotoxic $CD8^+$ T cells is required for their recruitment into the tumor microenvironment to produce effective antitumor immunity (33). These findings may explain the worse outcome observed in the clinical trial using the LTB_4 receptor antagonist. Future studies using the $BLT^{-/-}$ mice in our model would test the role of this receptor.

In addition to regulating the immune response, other mechanisms may contribute to increased tumor progression in 5-LO-KO mice. A recent study has identified one of the 5-LO products, 4-hydroxy-docosahexaenoic acid, as mediating the antiangiogenic effect of ω-3 fatty acids in a pathological retinal neovascularization model (23). Thus, the loss of 5-LO expression would be anticipated to increase angiogenesis. In fact, in our tumor model, we observed increased tumor microvessel density in the setting of 5-LO-KO. Furthermore, our eicosanoid profiling indicates that tumor-bearing lungs in 5-LO-KO mice have modestly increased levels of COX products. Previous reports have shown competition between COX and 5-LO for substrate, leading to shunting of arachidonic acid into 5-LO pathways in the setting of COX inhibitors (35). We would propose that in cells of the tumor microenvironment, the loss of 5-LO expression as occurs in the 5-LO-KO mice results in greater availability of arachidonic acid for COX pathways, leading to the observed increases in PG production, which could contribute to increased cancer progression in the setting of 5-LO KO. In addition to leukotrienes, 5-LO is critical for the production of proresolving lipid mediators (36). These molecules have been actively studied in vascular, airway, and dermal pathologies, but their role in lung cancer is not well defined, and further investigation is warranted. Although we have not observed significant differences in myeloid cells in the TME in the setting of 5-LO KO, leukotrienes, in particular LTB_4, are potent chemoattractants for myeloid cells (5). It has been reported that genetic deficiency of 5-LO in inflammatory and immune cells results in a shift of the cytokine profile toward Th2/M2 (37). Such shifts would predict a switch toward a tumor-promoting activation program in the TME, thus accelerating tumor progression in the setting of 5-LO deficiency. With regard to studies indicating an antitumorigenic role of 5-LO in cancer cells, it is likely that the same pathway plays opposing roles in cancer cells versus the tumor microenvironment. We have previously shown this for the nuclear receptor peroxisome proliferator-activated receptor γ, in which peroxisome proliferator-activated receptor γ activation in cancer cells inhibits tumor initiation, whereas activation in macrophages has tumor-promoting effects (15).

Finally, our current study examining the 5-LO pathway and our previous study examining tumor progression in $cPLA_2$ KO mice underscore the complexity of these pathways. In the setting of $cPLA_2$ deficiency, all eicosanoid production, both COX and 5-LO products, by the TME was ablated (16), and we observed decreased tumor progression (17). In this study, selective ablation of 5-LO products, but retention, and potentially increased COX products resulted in enhanced progression. This would suggest that in the developing tumor, there are multiple eicosanoids that have opposing effects on cancer progression. The net effect, leading to either progression or inhibition of tumor growth, will depend on this balance. These effects are likely mediated through different mechanisms, with COX products acting at least in part directly on cancer cells, whereas 5-LO products such as LTB_4 regulate the immune response. Thus, our data underscore the need for a better understanding of the complex role that eicosanoids play in the progression of lung cancer to design better therapeutic agents.

Acknowledgments

We thank the members of the University of Colorado Cancer Center Flow Cytometry Core for assistance with the flow cytometry.

Disclosures

The authors have no financial conflicts of interest.

References

1. Reungwetwattana, T., and G. K. Dy. 2013. Targeted therapies in development for non-small cell lung cancer. *J. Carcinog.* 12: 22.
2. Joyce, J. A., and J. W. Pollard. 2009. Microenvironmental regulation of metastasis. *Nat. Rev. Cancer* 9: 239–252.
3. Kenny, P. A., G. Y. Lee, and M. J. Bissell. 2007. Targeting the tumor microenvironment. *Front. Biosci.* 12: 3468–3474.
4. Cho, W. C., C. K. Kwan, S. Yau, P. P. So, P. C. Poon, and J. S. Au. 2011. The role of inflammation in the pathogenesis of lung cancer. *Expert Opin. Ther. Targets* 15: 1127–1137.
5. Peters-Golden, M., and W. R. Henderson, Jr. 2007. Leukotrienes. *N. Engl. J. Med.* 357: 1841–1854.
6. Pidgeon, G. P., J. Lysaght, S. Krishnamoorthy, J. V. Reynolds, K. O'Byrne, D. Nie, and K. V. Honn. 2007. Lipoxygenase metabolism: roles in tumor progression and survival. *Cancer Metastasis Rev.* 26: 503–524.

7. Steinhilber, D., A. S. Fischer, J. Metzner, S. D. Steinbrink, J. Roos, M. Ruthardt, and T. J. Maier. 2010. 5-lipoxygenase: underappreciated role of a pro-inflammatory enzyme in tumorigenesis. *Front. Pharmacol.* 1: 143.
8. Schwab, J. M., and C. N. Serhan. 2006. Lipoxins and new lipid mediators in the resolution of inflammation. *Curr. Opin. Pharmacol.* 6: 414–420.
9. Saif, M. W., H. Oettle, W. L. Vervenne, J. P. Thomas, G. Spitzer, C. Visseren-Grul, N. Enas, and D. A. Richards. 2009. Randomized double-blind phase II trial comparing gemcitabine plus LY293111 versus gemcitabine plus placebo in advanced adenocarcinoma of the pancreas. *Cancer J.* 15: 339–343.
10. Edelman, M. J., D. Watson, X. Wang, C. Morrison, R. A. Kratzke, S. Jewell, L. Hodgson, A. M. Mauer, A. Gajra, G. A. Masters, et al. 2008. Eicosanoid modulation in advanced lung cancer: cyclooxygenase-2 expression is a positive predictive factor for celecoxib + chemotherapy–Cancer and Leukemia Group B Trial 30203. *J. Clin. Oncol.* 26: 848–855.
11. Jänne, P. A., L. Paz-Ares, Y. Oh, C. Eschbach, V. Hirsh, N. Enas, L. Brail, and J. von Pawel. 2014. Randomized, double-blind, phase II trial comparing gemcitabine-cisplatin plus the LTB4 antagonist LY293111 versus gemcitabine-cisplatin plus placebo in first-line non-small-cell lung cancer. *J. Thorac. Oncol.* 9: 126–131.
12. Chen, Y., Y. Hu, H. Zhang, C. Peng, and S. Li. 2009. Loss of the Alox5 gene impairs leukemia stem cells and prevents chronic myeloid leukemia. *Nat. Genet.* 41: 783–792.
13. Cheon, E. C., K. Khazaie, M. W. Khan, M. J. Strouch, S. B. Krantz, J. Phillips, N. R. Blatner, L. M. Hix, M. Zhang, K. L. Dennis, et al. 2011. Mast cell 5-lipoxygenase activity promotes intestinal polyposis in APCDelta468 mice. *Cancer Res.* 71: 1627–1636.
14. Cheon, E. C., M. J. Strouch, S. B. Krantz, M. J. Heiferman, and D. J. Bentrem. 2012. Genetic deletion of 5-lipoxygenase increases tumor-infiltrating macrophages in Apc(Delta468) mice. *J. Gastrointest. Surg.* 16: 389–393.
15. Li, H., A. L. Sorenson, J. Poczobutt, J. Amin, T. Joyal, T. Sullivan, J. T. Crossno, Jr., M. C. Weiser-Evans, and R. A. Nemenoff. 2011. Activation of PPARγ in myeloid cells promotes lung cancer progression and metastasis. *PLoS One* 6: e28133.
16. Poczobutt, J. M., M. Gijon, J. Amin, D. Hanson, H. Li, D. Walker, M. Weiser-Evans, X. Lu, R. C. Murphy, and R. A. Nemenoff. 2013. Eicosanoid profiling in an orthotopic model of lung cancer progression by mass spectrometry demonstrates selective production of leukotrienes by inflammatory cells of the microenvironment. *PLoS One* 8: e79633.
17. Weiser-Evans, M. C., X. Q. Wang, J. Amin, V. Van Putten, R. Choudhary, R. A. Winn, R. Scheinman, P. Simpson, M. W. Geraci, and R. A. Nemenoff. 2009. Depletion of cytosolic phospholipase A2 in bone marrow-derived macrophages protects against lung cancer progression and metastasis. *Cancer Res.* 69: 1733–1738.
18. Weidner, N. 1995. Current pathologic methods for measuring intratumoral microvessel density within breast carcinoma and other solid tumors. *Breast Cancer Res. Treat.* 36: 169–180.
19. Lone, A. M., and K. Taskén. 2013. Proinflammatory and immunoregulatory roles of eicosanoids in T cells. *Front. Immunol.* 4: 130.
20. Duan, M., W. C. Li, R. Vlahos, M. J. Maxwell, G. P. Anderson, and M. L. Hibbs. 2012. Distinct macrophage subpopulations characterize acute infection and chronic inflammatory lung disease. *J. Immunol.* 189: 946–955.
21. Gautier, E. L., T. Shay, J. Miller, M. Greter, C. Jakubzick, S. Ivanov, J. Helft, A. Chow, K. G. Elpek, S. Gordonov, et al; Immunological Genome Consortium. 2012. Gene-expression profiles and transcriptional regulatory pathways that underlie the identity and diversity of mouse tissue macrophages. *Nat. Immunol.* 13: 1118–1128.
22. Janssen, W. J., L. Barthel, A. Muldrow, R. E. Oberley-Deegan, M. T. Kearns, C. Jakubzick, and P. M. Henson. 2011. Fas determines differential fates of resident and recruited macrophages during resolution of acute lung injury. *Am. J. Respir. Crit. Care Med.* 184: 547–560.
23. Sapieha, P., A. Stahl, J. Chen, M. R. Seaward, K. L. Willett, N. M. Krah, R. J. Dennison, K. M. Connor, C. M. Aderman, E. Liclican, et al. 2011. 5-Lipoxygenase metabolite 4-HDHA is a mediator of the antiangiogenic effect of ω-3 polyunsaturated fatty acids. *Sci. Transl. Med.* 3: 69ra12.
24. Wang, D., and R. N. Dubois. 2010. Eicosanoids and cancer. *Nat. Rev. Cancer* 10: 181–193.
25. Buczynski, M. W., D. S. Dumlao, and E. A. Dennis. 2009. Thematic Review Series: Proteomics. An integrated omics analysis of eicosanoid biology. *J. Lipid Res.* 50: 1015–1038.
26. Keith, R. L., Y. E. Miller, Y. Hoshikawa, M. D. Moore, T. L. Gesell, B. Gao, A. M. Malkinson, H. A. Golpon, R. A. Nemenoff, and M. W. Geraci. 2002. Manipulation of pulmonary prostacyclin synthase expression prevents murine lung cancer. *Cancer Res.* 62: 734–740.
27. Yuan, H., M. Y. Li, L. T. Ma, M. K. Hsin, T. S. Mok, M. J. Underwood, and G. G. Chen. 2010. 15-Lipoxygenases and its metabolites 15(S)-HETE and 13(S)-HODE in the development of non-small cell lung cancer. *Thorax* 65: 321–326.
28. Ghosh, J., and C. E. Myers. 1998. Inhibition of arachidonate 5-lipoxygenase triggers massive apoptosis in human prostate cancer cells. *Proc. Natl. Acad. Sci. USA* 95: 13182–13187.
29. Ding, X. Z., P. Iversen, M. W. Cluck, J. A. Knezetic, and T. E. Adrian. 1999. Lipoxygenase inhibitors abolish proliferation of human pancreatic cancer cells. *Biochem. Biophys. Res. Commun.* 261: 218–223.
30. Ding, X. Z., W. G. Tong, and T. E. Adrian. 2003. Multiple signal pathways are involved in the mitogenic effect of 5(S)-HETE in human pancreatic cancer. *Oncology* 65: 285–294.
31. Tong, W. G., X. Z. Ding, M. S. Talamonti, R. H. Bell, and T. E. Adrian. 2005. LTB4 stimulates growth of human pancreatic cancer cells via MAPK and PI-3 kinase pathways. *Biochem. Biophys. Res. Commun.* 335: 949–956.
32. Goodarzi, K., M. Goodarzi, A. M. Tager, A. D. Luster, and U. H. von Andrian. 2003. Leukotriene B4 and BLT1 control cytotoxic effector T cell recruitment to inflamed tissues. *Nat. Immunol.* 4: 965–973.
33. Sharma, R. K., Z. Chheda, V. R. Jala, and B. Haribabu. 2013. Expression of leukotriene B_4 receptor-1 on $CD8^+$ T cells is required for their migration into tumors to elicit effective antitumor immunity. *J. Immunol.* 191: 3462–3470.
34. Tager, A. M., S. K. Bromley, B. D. Medoff, S. A. Islam, S. D. Bercury, E. B. Friedrich, A. D. Carafone, R. E. Gerszten, and A. D. Luster. 2003. Leukotriene B4 receptor BLT1 mediates early effector T cell recruitment. *Nat. Immunol.* 4: 982–990.
35. Ganesh, R., D. J. Marks, K. Sales, M. C. Winslet, and A. M. Seifalian. 2012. Cyclooxygenase/lipoxygenase shunting lowers the anti-cancer effect of cyclooxygenase-2 inhibition in colorectal cancer cells. *World J. Surg. Oncol.* 10: 200.
36. Serhan, C. N. 2014. Pro-resolving lipid mediators are leads for resolution physiology. *Nature* 510: 92–101.
37. DiMeo, D., J. Tian, J. Zhang, S. Narushima, and D. J. Berg. 2008. Increased interleukin-10 production and Th2 skewing in the absence of 5-lipoxygenase. *Immunology* 123: 250–262.